

4D CT Scan Generation of Lung from Physical Simulation of Pulmonary Motion

Pierre-Frédéric Villard, Michaël Beuve, Behzad Shariat
LIRIS, bat Nautibus, 8 bd Niels Bohr, 69622 Villeurbanne CEDEX, FRANCE
pierre-frederic.villard@liris.univ-lyon1.fr

Abstract

Cancer treatments by ionising beam need accurate tumour targeting, which is difficult for lung cancer, due to breathing motions. We propose here to provide physicians with 3D + time CT scan of lung from a physically based simulation of respiratory organs motion.

1 Introduction

Radiation treatments like radiotherapy and hadrontherapy are efficient techniques to definitely reduce local cancerous tumours. However, such techniques need an accurate knowledge of organ positions to correctly target tumours. We focus here on lung motion where tumour position fluctuates due to breathing process. To deal with motion, cancer therapies mainly consist in applying safety margins, due to the lack of information preventing from any better solution. Physically-based modelling techniques, currently used in computer graphics, aim precisely at simulating soft tissues behaviour. However, geometrical informations about lung deformation is not the most useful for physicians. They need to have lung tomographic density evolution. Hence, we propose here to construct a bridge between such simulations and the therapy: a tool to convert motion into dynamic CT scan.

2 Survey

2.1 therapeutic treatment strategies

To manage pulmonary motion during treatments, several strategies can be established. Breath gating holds lung into a well determined volume. This is finally equivalent to a static treatment [7]. Beam gating allows to irradiate tumours for a limited domain positions. Tracking aims at conforming the beam to tumours despite the motion, allowing a free patient breathing. Even presently, the knowledge of motions could improve the quality of treatments planning by optimising margins. In [5], an environment simulation is presented in which the time-dependent effect of target motion can be calculated with dynamical ion beams.

2.2 Physically based simulations

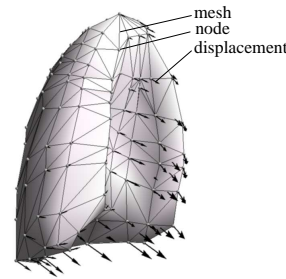


Figure 1: FEM result: node displacements

Physically-based modelling attempts to mimic as possible a natural phenomena with physical laws. For most of complex systems, numerical simulations are necessary to solve the associated equations. Consequently, a process of discretization

is applied and consists, in the case of motion, in meshing the object and predicting the displacement at each node (Cf Figure.1). To simulate lung inflation, three approaches has been commonly explored: Mass-spring system ([4], [6], [2]), particle system ([1]) and Finite element method ([3], [2]).

3 Our Methodology

The aim of this work is to convert the time-dependent displacements of each lung mesh node $\{U\}$ into a 3D+t CT scan defined by the CT scan at initial time. The algorithm, illustrated by Figure.2, is essentially a loop over time. Starting from a given CT scan at t_0 and a mesh G_0 we calculate for each node i the density $\{\rho_0\}$. For each simulation time step t_j , the predicted displacements provide us with the geometry G_j and then node density $\{\rho_j\}$. A CT scan can finally be generated at any time t_i with the help of an iterative process. Our method consists mainly in three tools: computing a CT scan with matter density, optimising the model mesh resolution and computing for each time step the new matter density.

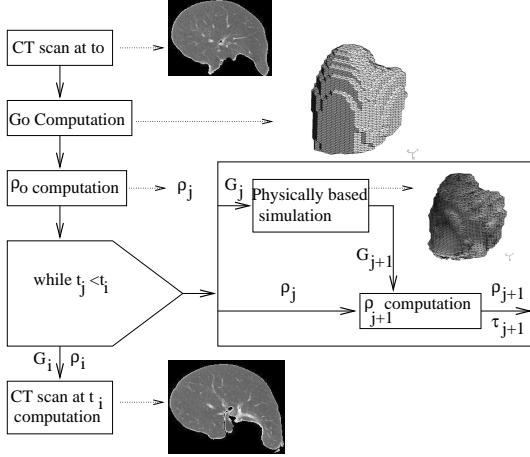


Figure 2: CT scan generation principles

3.1 CT scan Computation with matter density

A 3D CT scan is composed of a set of volume elements (voxels) affected with numbers characterising their ability to absorb photons: the Hounsfield

density. Practically, this value not only depends on matter density and chemical composition but the whole instrumentation chain plays a role and a calibration is necessary to reach accurate absolute values. Indeed, due to the beam straggling, and due to the realistic nature of sensors as well as all the stages of image processing, the Hounsfield density of a voxel is likely to depend on the characteristics of neighbouring voxels. Moreover, the final Hounsfield density of a voxel results from an average over the voxel of all Hounsfield density inside the voxel. Finally we model all this process by a combination of convolution and average. By mesh discretization a matrix relation could be found to link matter density $\rho_M[i]$ of node i with Hounsfield density $\rho_H[l]$ of a voxel l with a matrix $A[l][i]$:

$$\rho_H[l] = A[l][i] \cdot \rho_M[i] \quad (1)$$

To compute the initial node density, matrix A is inverted and applied to initial Hounsfield density matrix.

3.2 Mesh Resolution Optimisation

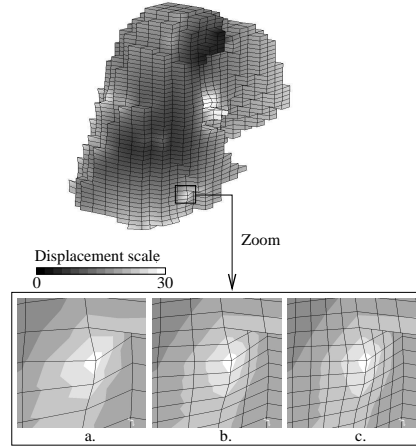


Figure 3: Mesh subdivision. Subdivision number for zoomed details: **a.**: 1 - **b.**: 2 - **c.**: 4

Mesh resolution for the physical simulation is not chosen to be very high in order to reduce memory needs while CT scan images are defined with better resolution. Typically in our case, finite element mesh resolution of element is $15 \times 15 \times 10$ mm hexahedrons while CT scan voxel resolution is $0.9375 \times 0.9375 \times 5$ mm. To link Simulation to

CT scan informations, sampling must be optimised (Cf Figure.3). Practically, each hexahedron is subdivided into eight new hexahedrons of same size. The mesh optimisation will depend on the number of the subdivision optimisation.

3.3 Node Density Computation

The only known quantity to calculate the density is the displacement, which has to be converted. The key point of our approach is an iterative integration of mass conservation equation (Equation.2):

$$\frac{\partial \rho_M}{\partial t} + \text{div}(\rho_M \cdot \mathbf{V}) = 0 \quad (2)$$

The interest of this equation is the presence of the velocity \mathbf{V} that can be replaced by displacement with time integration over a short time. Knowing the displacement for a short time step, one can calculate the variation $\Delta \rho$ of density. Practically, it consists in inserting in equation (2) the following discretized density expression stemming from finite element method.

$$\rho(\mathbf{P}, t_i) = \sum_{j \in E_i} N_j(\mathbf{P}) \cdot \rho(\mathbf{P}_j, t_i) \quad (3)$$

where E_i represent the mesh elements, $N_j(\mathbf{P})$ is the interpolation function at the node j . Then, $\Delta \rho = \rho(\mathbf{P}, t_i + \Delta t) - \rho(\mathbf{P}, t_i)$ for any point P in element E_i reads:

$$\Delta \rho \approx - \sum_{j, j'} \rho(\mathbf{P}_j, t_i) \cdot \text{div}(N_j(\mathbf{P}) \cdot N_{j'}(\mathbf{P}) \cdot \mathbf{U}_i(\mathbf{P}_{j'})) \quad (4)$$

Finally equation (4), provided the time step is small, allows us to calculate the $\Delta \rho$ from the simple knowledge of node position, node densities at previous state and node displacements over the time step.

4 validation and results

In previous sections we presented the whole process to convert a lung deformation simulation into a 4D CT scan. The conversion necessitates many intermediate calculations that can alter the quality of the obtained results. In order to detect any possible computation artifacts due to all the integrations or other calculations, we present now a series of tests to check the qualitative validity as well as the quantitative validity of each conversion step.

4.1 Implementation

The simulation parameters are the following : first geometry is extracted from the same patient, characterised by 10231 points and 29902 elements. Lung bounding box dimensions are $240 \text{ mm} \times 180 \text{ mm} \times 245 \text{ mm}$. Our numerical simulations have been carried out with the Code Aster finite element software. The tests have been realised on a Intel(R) Xeon(TM) CPU 3.20GHz with 2GB memory.

4.2 Density continuity

This stage consists in qualitatively validating the spatial evolution of the matter density . Figure 4 shows a continuous representation of density values computed on mesh nodes during the first time step. It is a smoothing function that uses the Gouraud method, i.e. colour interpolations.

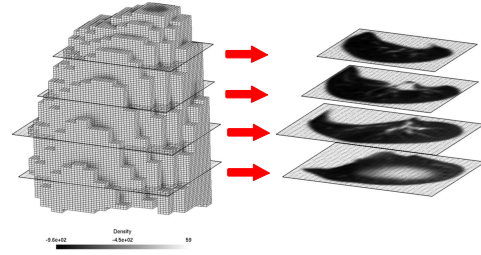


Figure 4: Checking of matter density continuity with example slices

The obtained mesh is constituted of density values where extracted slices show a good 3D continuity in time. There is neither boundary aberration nor problems associated to mesh optimisation. Moreover, anatomical structures can clearly be noticed and this 3D CT scan is in fully adequacy with the given initial 3D CT scan.

4.3 Mass conservation

The iterative process may induce cumulated error due to the approximation in the time integration of density. To perform a quantitative evaluation we defined a mass loss error at each time step by:

$$\begin{aligned} \text{Error}[\%] &= \frac{\text{mass}_{\text{theoretical}} - \text{mass}_{\text{computed}}}{\text{mass}_{\text{theoretical}}} \times 100 \end{aligned} \quad (5)$$

In our simulation, the time step corresponds to one load step of the physical simulation. Results of tests gathered in Table.1, show that our method is quite correct since mass-loss error is always bellow 0.2%. Our tool ensures well the mass conservation and there is no numerical artefact.

Time step	Mass loss in [%]
1	0.021
2	0.04
3	0.056
4	0.07
5	0.082
6	0.093
7	0.101
8	0.109
09	0.114
10	0.119

Table 1: Mass conservation error evolution

4.4 CT scan convolution

The following test consists in checking if our scanner convolution is correct. The result given in the Figure 5 shows a CT scan calculated after one time step. We observe low grey levels at the lung border due to the smoothing effect of convolution. No artefact can be noted.

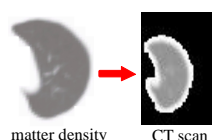


Figure 5: Comparison for the same slice of the CT scan and the matter density

5 conclusion

We proposed here a model for generation of 3D + time CT scan. A great interest of our approach is that the simulated-displacement data could be calculated with any kind of physically based techniques. The presented work provides physicians

with standard images useful to appreciate organ motions and to incorporate them into a treatment planning platform.

Currently, comparing our simulated CT scan with the reality, we will add more details in our simulation (heterogeneity, ...), if necessary for therapy accuracy. At the same time, dosimetry will be included into our model with respect to physical laws.

References

- [1] M. Amrani. *Modelling and simulating deformable objects*. PhD thesis, Université Claude Bernard Lyon, 2002.
- [2] V. Baudet, P-F. Villard, F. Jaillet, M. Beuve, and B. Shariat. Towards accurate tumour tracking in lungs. *IEEE, Mediviz, Conference on Information Visualization*, pages 338–343, 2003.
- [3] Q. Grimal, A. Watzky, and S. Naili. Non-penetrating impact on the thorax : a study of the wave propagation. *Comptes Rendus de l'Académie des Sciences*, IIb(329):655–662, 2001.
- [4] J. Kaye, D.N.Metaxas, and F.P.Primiano. A 3D virtual environment for modeling mechanical cardiopulmonary interactions. *National Library of Medicine and the Philadelphia VAMC*, 1(LM-4-3515), 1998.
- [5] Q. Li, S.O. Groezinger, T. Haberer, E. Rietzel, and G. Kraft. Online compensation for target motion with scanned particle beams: simulation environment. *Physics in Medicine and Biology*, 49(14):3029–3046, 2004.
- [6] E. Promayon. *Modelling and simulation of the respiration*. PhD thesis, Université Joseph Fourier de Grenoble, 1997.
- [7] J. W. Wong and al. The use of active breathing control (ABC) to reduce margin for breathing motion. *Int. J. Radiation Oncology Biol. Phys.*, 44(4):911–919, 1999.